Transforming the near-bit sensor into a reliable pilot for seismic while drilling

Anton Egorov and Pavel Golikov, Aramco Research Center - Moscow, Aramco Innovations LLC;
Ilya Silvestrov and Andrey Bakulin, EXPEC Advanced Research Center, Saudi Aramco

Summary

Seismic-while-drilling (SWD) success hinges on recording a reliable drill-bit source function. Top-drive sensors can provide an acceptable pilot with GPS synchronized timing. Downhole memory-based vibration tools have the potential to deliver a better pilot. Their clocks are unsynchronized, leading to a large drift that is unacceptable for SWD. We demonstrate a methodology to resolve this issue by combining the recording of the downhole sensor with the top-drive sensor recordings. We propose a two-step procedure for drift correction. The first step is a novel automated linear drift correction, which acts as an alternative to existing semi-manual approaches used in drilling. The second step is a time-variant cross-correlation between two sensors. We demonstrate the new method on an extensive field dataset. Besides, we compare the near-bit and top-drive recorded accelerations as source functions for SWD.

Introduction

In seismic while drilling (SWD), the vibrations emanating from the drill-bit source are recorded by seismic sensors on the surface or in a nearby well. These recordings are later used to produce an image of the subsurface and characterize its properties. There are several approaches for the processing of SWD data. Most of these approaches require an estimate of the drill bit's source function. In some cases, it may be possible to estimate it directly from the surface geophones' recordings without the need for additional sensors (Goertz et al., 2020). Still, in most cases, the source function is directly recorded by accelerometers located either on the top drive or downhole (Poletto and Miranda, 2004). The time series recorded by these sensors are directly used for correlation and deconvolution of SWD data.

The top-drive recorder is synchronized to the GPS clock and can be directly used for data processing. The near-bit memory-based sensors are widely used to measure drilling vibrations. They rely on the internal clock, which is typically unsynchronized and susceptible to large temperature-dependent drift. Drilling applications of memory-based sensors rely on semi-manual clock synchronization and drift corrections. The traditional workflow involves identifying similar characteristic events on the downhole data and surface RPM (drillstring revolutions per minute) curves and aligning these events by introducing a correction into the near-bit clock (Figure 1a). This usually leads to a correction with an error of a few seconds, which is suitable for drilling dynamics analysis but is not enough for SWD. To reduce an error to a few milliseconds required by SWD, time-variant cross-correlation (TVCC) analysis is often applied (Naville et al., 2004).

We suggest a replacement for the semi-manual drift correction procedure. This replacement is an optimization-based method of linear drift estimation, which is then followed by TVCC for SWD. We test the suggested method on a dataset acquired during a field test of the DrillCAM system. The system recorded three continuous datasets from the surface down to 10,000 ft: top-drive sensor, near-bit accelerometer, and surface geophone spread (Bakulin et al., 2020).

After conducting sensor alignment, we perform a modeling-based analysis of the top-drive and near-bit sensor autocorrelations. For each drilling segment, we create a 1D model of the bottomhole assembly (BHA) and drillstring and conduct wave propagation with a matrix propagator/transmission line algorithm (Poletto et al., 2001). We then compute the autocorrelations of the synthetic data and compare them to field data autocorrelations.

Finally, after performing the alignment and autocorrelation analysis, we use the aligned top-drive and downhole source functions to compute the SWD reverse vertical seismic profile (VSP) gathers, comparing their quality.

Method

The first step of our clock drift removal methodology is an optimization-based procedure, which estimates and corrects the linear component of the clock drift. We introduce two parameters, drift d and shift s, which describe the relationship between the times recorded by the two clocks:

$$t^{td} = (1+d)t^{nb} + s; \qquad t^{nb} = (t^{td} - s)/(1+d).$$

Here, t^{td} and t^{nb} are the top-drive and near-bit time vectors. The top-drive time acts as a reference; the near-bit time is to be aligned with it. These vectors have the same origin, which in our case is the moment of the battery installation in the downhole sensor. Zero values of d and s mean that the downhole clock is accurate.

When surface and downhole RPM curves are available, we can form the following misfit for the estimation of d and s. High-frequency downhole RPM is typically captured by the downhole tool in addition to vibrations. The minimization of the misfit function yields the optimal values $\hat{d}$ and $\hat{s}$, which provide alignment of the sensor clock:

$$J(d,s) = \sum_{t^{td}} \left(RPM^{td}(t^{td}) - RPM^{nb}\left(\frac{(t^{td}-s)}{(1+d)}\right)\right)^2;$$
$$\hat{d}, \hat{s} = argmin\, J(d,s).$$

If the RPM curves are unavailable for some reason, other common drilling parameters can be used for such alignment. We have found that top-drive and downhole energies computed directly from accelerometers' recordings in a large sliding window (e.g., 30 seconds) can be similarly used for the same purpose.

According to our experience, this linear drift removal procedure typically provides an accuracy of a few seconds. SWD requires higher accuracy, so we proceed to conduct the TVCC analysis to remove the remaining nonlinear drift (Naville et al., 2004).

After both steps are completed, we take the resulting top and downhole source functions and compute their deconvolved autocorrelations (Poletto and Miranda, 2004) in 30-second-long segments. We then stack these autocorrelations over one drillpipe length. For every resulting autocorrelation trace, we compute a synthetic counterpart using the matrix propagator algorithm, which takes the dimensions and properties of the BHA and drillpipes and models wave propagation in the drillstring.

Finally, the aligned source functions are used to compute reverse VSP seismic gathers. For this, the wave propagation time in the drillstring is computed from the multiples on autocorrelations and introduced into both sensors' recordings as a static correction to shift the recordings to true downhole source excitation time. This is followed by the correlation of the pilot sensors' recordings with the surface geophone data. The one-sided pilot deconvolution of the cross-correlations is performed to remove the anti-causal events on the seismic gather caused by the drillstring-related multiples.

Field data example – alignment

Figure 1a shows the surface and downhole RPM curves. Clock drift is evident from the surface (blue) and unaligned near-bit (orange) RPM. The suggested linear drift estimation procedure successfully estimates the drift and provides a correctly aligned downhole RPM (green). We use a constrained grid search method (we also found that simplex search provides similar results). The objective function computed on the grid is shown in Figure 1b. There is a single well-defined minimum of the objective function.

After the linear drift correction step, we conduct the TVCC analysis shown in Figure 2. We compute the cross-correlations of the top-drive and near-bit sensors recordings in 30-second-long windows and pick the maxima to identify the remaining drift (the maxima are highlighted in blue). One can observe that there is a remaining linear component of the drift after the first step, which is approximately 3.5 seconds over 1,500 minutes, but the nonlinear fluctuations of the drift are also present. The times of these picked cross-correlation maxima are used for the second step of the clock alignment.

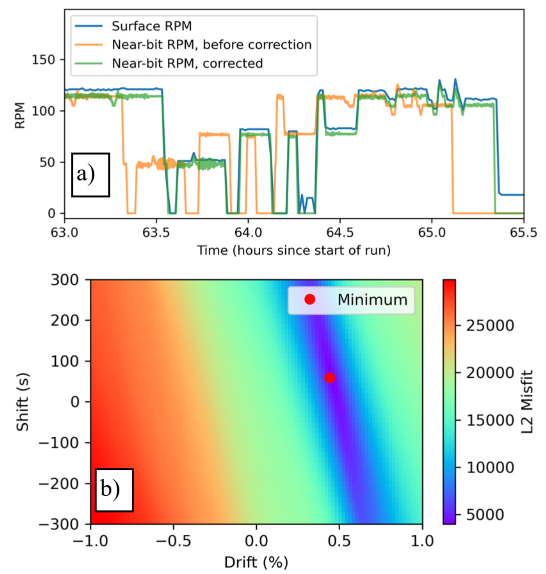

Figure 1: Surface (blue) and downhole RPM curves before (orange) and after (green) alignment (a) and the alignment objective function computed for a range of values of drift and shift (b).

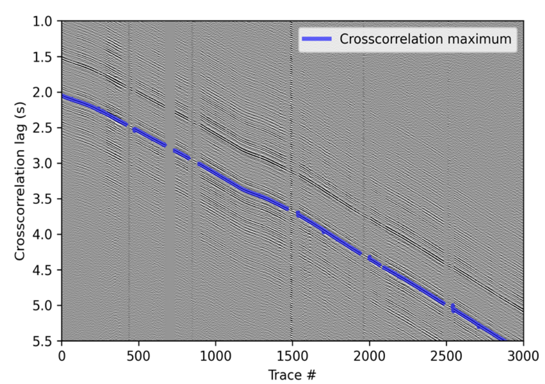

Figure 2: Cross-correlations of the top-drive and near-bit accelerations after the first alignment step computed in 30-second-long windows. Crosscorrelation maxima are highlighted in blue.

Field data example – analysis of autocorrelations and seismic gathers

Figure 3 shows the comparison of the field and synthetic autocorrelations for the top-drive (a) and near-bit (b) sensors' recordings. Note the overall similarity of the field and synthetic autocorrelations. The events observed on the autocorrelations can be attributed to the interaction of the bit vibration with the different segments of the drillstring and BHA. The interpretation of the events on some characteristic lags of autocorrelations is shown in Figures 3c and 3d. It can be observed that the multiples are not present in the top-drive autocorrelations for the deeper part of the well below 6000 ft. The sections above 6000 ft were mainly drilled with roller cone bits and a large-diameter PDC bit. The segments below 6000 ft were drilled with smaller-diameter polycrystalline diamond (PDC) bits, which are known to be less noisy and therefore less favorable for SWD (Poletto and Miranda, 2004). The downhole autocorrelations contain the multiples, which is probably related to the higher signal-to-noise ratio of the downhole tool – it is located closer to the bit. It is not sensitive to rig noise, unlike the top-drive sensor. It more accurately detects the low-amplitude extensional vibrations of the PDC bits.

Figure 4 displays a comparison of the reverse VSP gathers acquired with the top-drive and near-bit source functions. Similar events with the same arrival times can be observed on both gathers. There is a drastic difference in the signal-to-noise ratio. First arrivals are much cleaner on the gather obtained using the near-bit pilot source function. This also

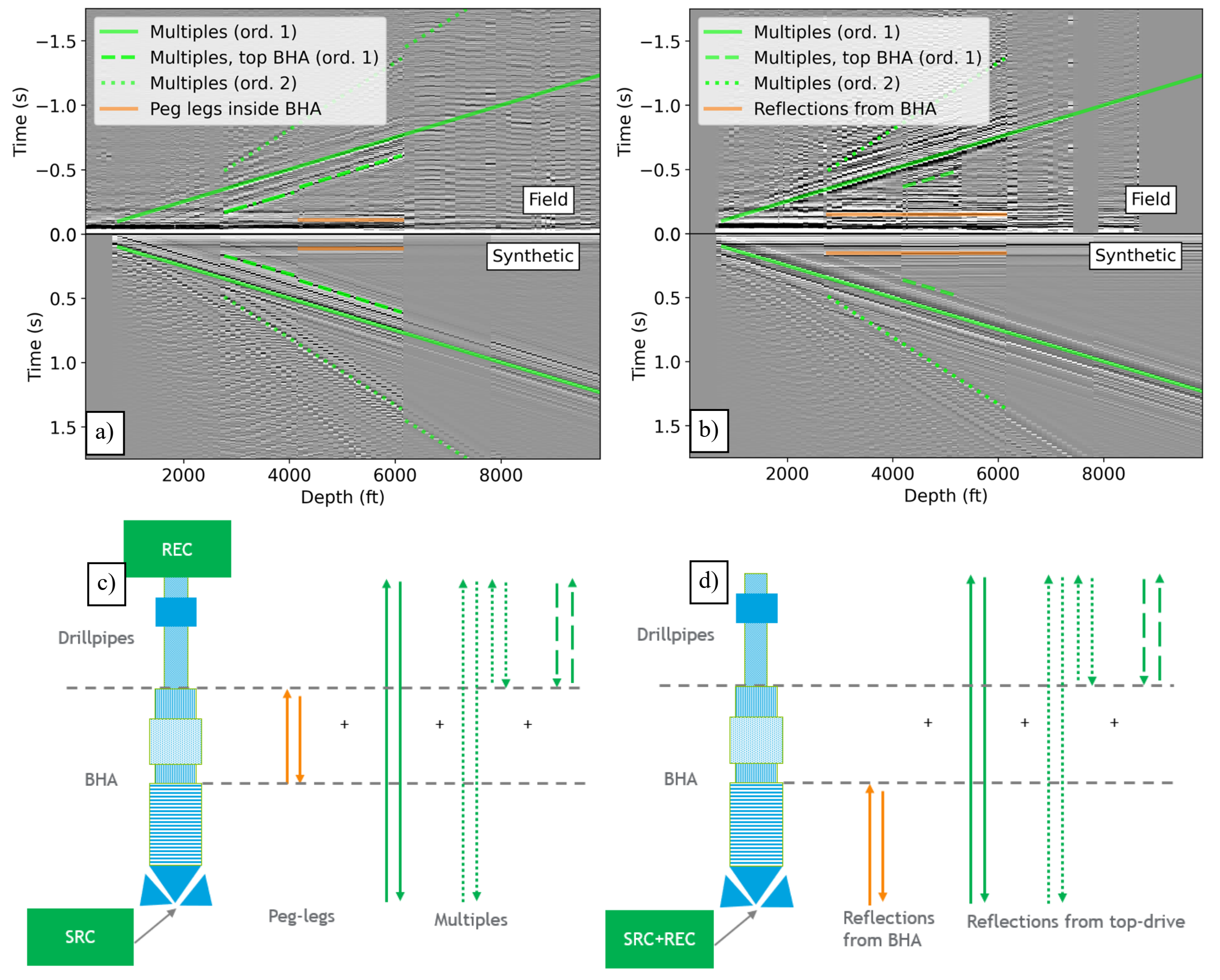

Figure 3: A comparison of field and synthetic autocorrelations for the top-drive (a) and near-bit (b) sensors' recordings and a schematic interpretation of some characteristic autocorrelation lags for top-drive (c) and near-bit (d) sensors.

can be explained by the higher signal-to-noise ratio of the pilot from the near-bit sensor.

Discussion

We demonstrate that the downhole sensor recording can be used for SWD even when the downhole sensor has significant clock drift. While initial correction can be done by aligning surface and downhole RPM, it is essential to note that the quality of the second step of drift correction depends on the goodness of cross-correlation between the near-bit and top-drive sensors. Thus, the top-drive sensor needs to be present throughout the whole acquisition. If the top-drive sensor breaks down – the near-bit drift correction immediately becomes impossible. Finally, with a long drillstring, extensional signals from the bit may become heavily attenuated, making cross-correlation unreliable. This could make alignment unfeasible for deeper sections. Top-drive-independent correction workflows are a part of our future research plan.

Conclusions

We show how to transform a near-bit sensor with a drifting clock into a reliable pilot for SWD. We come up with a two-step clock drift removal procedure for the near-bit sensor in SWD. The first step is a novel automatic optimization-based removal of linear drift that only requires surface RPM from the drilling recorder and downhole RPM from the near-bit tool. The second step conducts time-variant cross-correlation analysis with GPS-synchronized top-drive sensor. When applied to a field dataset, this methodology successfully estimates and removes the near-bit sensor's clock drift and provides the near-bit source function for SWD processing. Following the drift correction, we conduct a modeling-based analysis of top-drive and near-bit autocorrelations and obtain reverse VSP SWD gathers with top-drive and near-bit source functions. They show that the near-bit sensor provides a pilot capturing drillbit vibrations with higher fidelity and results in higher quality SWD gathers after processing.

Acknowledgments

We thank Flavio Poletto (OGS) for sharing his experience and advice during the study. We are thankful to Grant Corrie and Sahet Keshiyev (both of NOV) for fruitful discussion on existing alignment approaches for drilling optimization applications. We are grateful to Yue Du and Yujin Liu (both of the Aramco Research Center - Beijing) for their initial assessment of the synchronization issue in the considered field study. This paper also benefited from the constructive suggestions from Mustafa Al-Ali, Timur Zharnikov (both of the Aramco Research Center - Moscow), Emad Hemyari, and Robert Smith (both of Saudi Aramco).

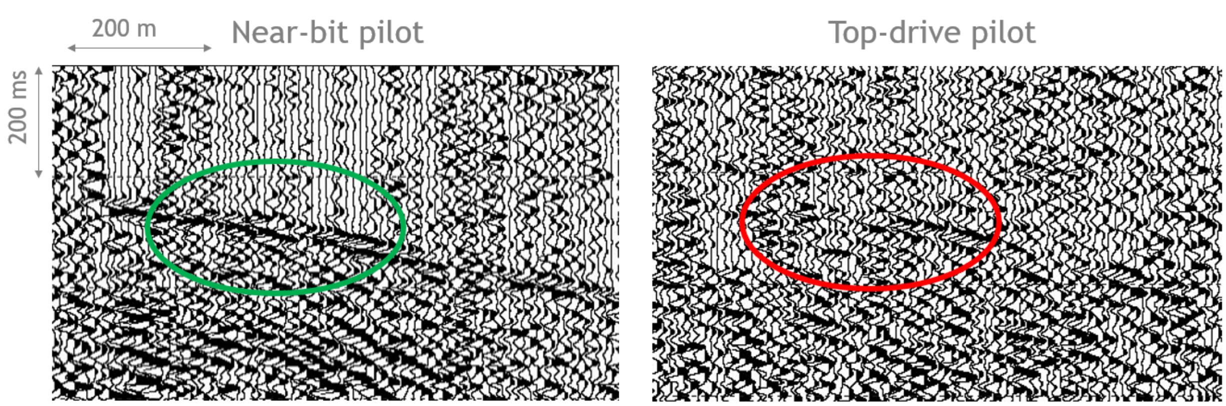

Figure 4: A comparision of the SWD reverse VSP gathers computed using near-bit (left) and top-drive (right) pilot source functions.

REFERENCES

Bakulin, A., A. Aldawood, I. Silvestrov, E. Hemyari, and F. Poletto, 2020, Seismic-while-drilling applications from the first DrillCAM trial with wireless geophones and instrumented top drive: The Leading Edge, **39**, 422–429, doi: https://doi.org/10.1190/tle39060422.1.

Goertz, A., B. Atkinson, T. Thiem, and E. V. Bergfjord, 2020, Reservoir imaging-while-drilling with PRM arrays: First Break, **38**, 77–83, doi: https://doi.org/10.3997/1365-2397.fb2020083.

Naville, C., S. Serbutoviez, A. Throo, O. Vincké, and F. Cecconi, 2004, Seismic While Drilling (SWD) Techniques with Downhole Measurements, Introduced by IFP and Its Partners in 1990-2000: Oil & Gas Science and Technology, **59**, 371–403, doi: https://doi.org/10.2516/ogst:2004027.

Poletto, F., M. Malusa, and F. Miranda, 2001, Numerical modeling and interpretation of drillstring waves: Geophysics, **66**, 1569–1581, doi: https://doi.org/10.1190/1.1487102.

Poletto, F., and F. Miranda, 2004, Seismic while drilling: Fundamentals of drill-bit seismic for exploration: Elsevier.